Original Article

Effect of Different Mini Implant Assisted Rapid Palatal Expansion (MARPE) Designs on Maxillary Protraction in Skeletal Class III malocclusion: An FEM Study

Ashik Suresh, Ajith Vallikat Velath, K. Sarika, Rahul Damodaran Prabha, N. K. Sapna Varma

Department of Orthodontics and Dentofacial Orthopedics, Amrita School of Dentistry, Amrita Vishwa Vidyapeetham, Kochi, Kerala, India

Abstract

Background: Four different designs of mini-implant-assisted rapid palatal expansion (MARPE) and protraction in nasomaxillary complex and mid-palatal sutures in late adolescent skeletal Class III malocclusion were compared using a three-dimensional finite element analysis. **Methods:** A finite element model of skull and related sutures was constructed using the computed tomography scan of a 16-year-old female patient with skeletal Class III and ANB of −2°. Four appliance designs: Type I: MARPE with palatal force, Type II: MARPE with buccal force, Type III: Hybrid hyrax with palatal force, and Type IV: Hybrid hyrax with buccal force. Protraction vectors were and analyzed using Ansys software (ANSYS 2021 R2). The displacement pattern of the nasomaxillary structures and the stress distribution in the sutures were examined in all four appliance designs. **Results:** All the appliance designs resulted in a forward movement of the maxilla, while Type I and III, which used palatal protraction force, caused the greatest forward displacement. In Type I, II, and III, along with forward movement, a clockwise rotation of maxilla was observed, while in Type IV, an anticlockwise rotation of maxilla was observed. Type I, II, and III resulted in higher stress distribution around the superior structures, while Type IV resulted in less stress distribution around the superior structures of maxilla. **Conclusion:** The forward displacement was enhanced when palatal plates were used to protract the maxilla. The effective appliance design for skeletal class III with open bite case was Type I, II, and III and Type IV for deep bite cases.

Keywords: *Finite element method, maxillary protraction, mini-implant-assisted rapid palatal expansion, skeletal class III*

Introduction

Management of complex skeletal Class III malocclusion often presents as a severe clinical challenge. Skeletal Class III malocclusion appears as combinations of retrusive maxilla with a decrease in effective length, increase in length of the mandible, increased anterior facial height, and dentoalveolar compensations such as proclined maxillary anteriors and retroclined mandibular anteriors.[1] Treatment options include orthognathic surgery, orthodontic camouflage therapy, and dentofacial orthopedic procedures employing protraction facemasks in growing patients.[2]

Maxillary deficiency in the sagittal plane is usually combined with or without skeletal transverse discrepancy. Maxillary protraction, along with maxillary expansion, is a popular treatment modality for correction of skeletal Class III malocclusion during the deciduous and mixed dentition periods. In cases with transverse discrepancy, rapid maxillary expansion (RME) is activated for skeletal expansion, and in patients without transverse discrepancy, rapid palatal expansion is given for loosening or mobilizing the circummaxillary sutures to provide a more effective protraction.[3,4]

Recent advances in skeletal anchorage system, enabled modifications of RME as a bone-borne appliance and hybrid hyrax appliance that can bring about true skeletal changes. The palatal bone has been found to be a safe skeletal anchorage site with a high rate of success. For the easier placement of the bone-anchored devices, Wilmes *et al*. developed the hybrid Hyrax, which is a tooth and bone-anchored device.[5] The expansion device is attached to the first molars and two mini-implants

How to cite this article: Suresh A, Velath AV, Sarika K, Prabha RD, Varma NK. Effect of different mini implant assisted rapid palatal expansion (MARPE) designs on maxillary protraction in skeletal class III malocclusion: An FEM study. Contemp Clin Dent 2024;15:27-34.

Submitted : 13-Sep-2023
Revised : 29-Oct-2023
Accepted : 19-Dec-2023
Published : 23-Mar-2024

Address for correspondence:
Dr. Ajith Vallikat Velath, Department of Orthodontics and Dentofacial Orthopedics, Amrita School of Dentistry, Amrita Vishwa Vidyapeetham, Kochi - 682 041, Kerala, India.
E-mail: ajithvv72@gmail.com

Access this article online

Website: https://journals.lww.com/cocd

DOI: 10.4103/ccd.ccd_428_23

Quick Response Code:

that are positioned in the anterior palate. The effects of a face mask and RME can be effectively explained using three-dimensional (3D) finite element method (FEM). The FEM analysis is a noninvasive technique for realistically investigating clinical scenarios and evaluating the pattern of displacement and stress distribution in various clinical procedures.

This study aimed to analyze the displacement and stress distribution in the maxillofacial complex during maxillary expansion and protraction using a bone-borne RME (four screw) and a hybrid hyrax (two screw) with two points of force application, i.e. buccal and palatal through 3D finite element analysis (FEA).

Methods

A finite element model was constructed using computed tomography (CT) scan of craniomaxillofacial complex of a patient (16-year-old female) with skeletal Class III malocclusion and ANB value of −2°.

Finite element analysis

The patient's CT image was converted into a computer-aided design model using MIMICS version 25.0 (Materialise, Leuven, Belgium) to create a 3D image. Each part was recreated layer on layer around the reference coordinates. To further refine the structures craniofacial bones, teeth, periodontal ligament (PDL), and sutures of the skull were segmented into a separate 3D model [Figure 1]. The craniomaxillary complex's reconstructed geometry was exported in STL file format. ANSYS 2021 R^2 was used to produce a quadratic tetrahedral element. The maximum element edge length after discretization is 1.2 mm and minimum is 0.6 mm for the maxilla, dentition, and alveolar bone. The remaining skull bones were 1.2 mm maximum size and near the sutures were sectioned into 0.25 mm tetrahedrons. A mesh convergence study is conducted with deformation as the output parameter. The model comprised 6517154 elements and 1163869 nodes after the study. The PDL, alveolar bone, and teeth were considered homogeneous and isotropic tissues. Based on previous studies, the thickness of sutures was 0.5 mm, separated into two layers, and the thickness of PDL was 0.2 mm.[6] The material properties of various structures of the craniofacial complex used in the study are explained in Table 1.[7]

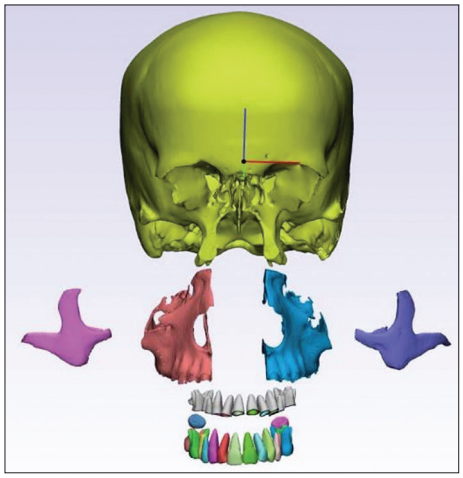

Figure 1: Segmented three-dimensional model

3D co-ordinates

Gautam *et al*.[2] reported the foramen magnum and forehead were fixed and employed as the origin point, with limited upward, downward, forward, backward, right, and left displacements [Figure 2]. The 3D co-ordinates were the X axis-transverse plane, Y axis–sagittal plane and Z axis–vertical plane. The X, Y, and Z axes were used to symmetrically distribute the load. Positive numbers on the X-axis indicate leftward movement, whereas negative values indicate rightward movement. Positive values on the Y-axis represent movement backward, whereas negative values represent movement ahead. Positive values on the Z-axis represent upward motions, while negative values represent downward movements of the maxillary complex.

Appliance design

Based on 3D data, four appliances were designed as 3D finite element models: the bone-borne RME with palatal pull (Type I), the bone-borne RME with buccal pull (Type II), the hybrid hyrax with palatal pull (Type III), and the hybrid hyrax with buccal pull (Type IV). The projection approach was used to merge these models with the skull model.

Type I: mini-implant-assisted rapid palatal expansion (MARPE) with hooks on the palatal side for maxillary protraction using face mask was used. Four

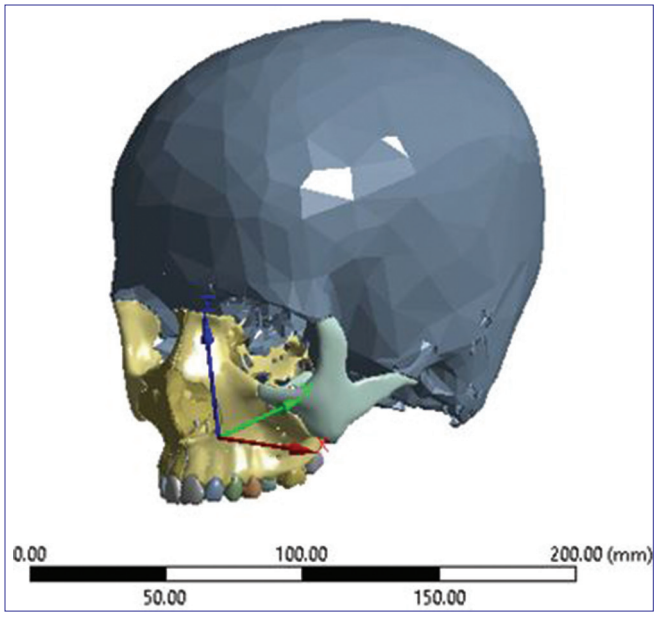

Figure 2: 3D co ordinates: X axis transverse plane, Y axis–sagittal plane and Z axis–vertical plane

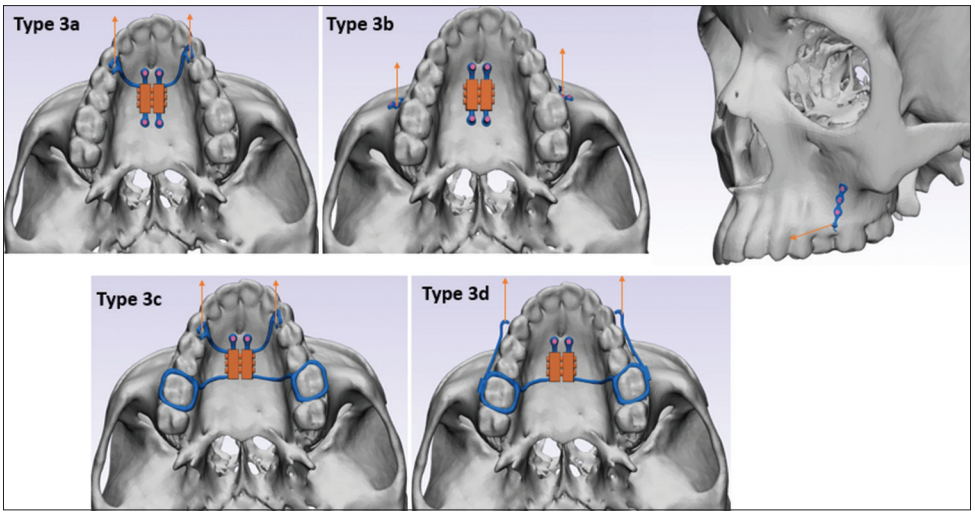

Figure 3: Appliance Designs. (a) Mini-implant assisted rapid palatal expansion (MARPE) with palatal hooks (Type I), (b) MARPE with mini plate (Type II), (c) Hybrid hyrax with palatal hooks (Type III), (d) Hybrid hyrax with buccal hooks and arrow represents the point of force application

mini-screws (diameter: 2 mm; length: 8 mm) spaced 2 mm apart from the midpalatal suture were used to attach the RME to the palate. The palatal hook for maxillary protraction was positioned between the first premolar and canine at the gingival level [Figure 3a].

Type II: MARPE with hooks on the buccal side for maxillary protraction using face mask was used. The RME was fixed to the palate the same as in Type I. Mini plates for maxillary protraction were fixed with mini-screws (diameter: 2 mm and length: 8 mm) on the infrazygomatic are between the second premolar and molar area [Figure 3b].

Type III: Hybrid hyrax with hooks on the palatal side for maxillary protraction using face mask. The RME was fixed to the palate with 2 mini-implants on the anterior side and on the molars posteriorly. The palatal hook was placed the same as in Type I [Figure 3c].

Type IV: Hybrid hyrax with hooks on the buccal side for maxillary protraction using the face mask. The RME was fixed to the palate same as in Type III. The hooks for maxillary protraction are soldered to the molar band posteriorly and extend 2 mm below to the alveolar crest anteriorly between the canine and first premolar [Figure 3d].

To avoid tension around the miniscrews, they were firmly attached to the bone by sharing nodes. Using materialize 3-matic, a computer-aided design program, the mini screws, expander, and miniplates were modeled and positioned using the CT images as positioning guides to suit the specifics of the situation. To avoid obstructing the resulting movement, the expanders were unfixed in the Y and Z directions and activated horizontally for 0.25 mm at the level of the expansion screw in the X direction.[8] To reduce the anticlockwise rotation brought on by maxillary protraction below the center of resistance, a protraction

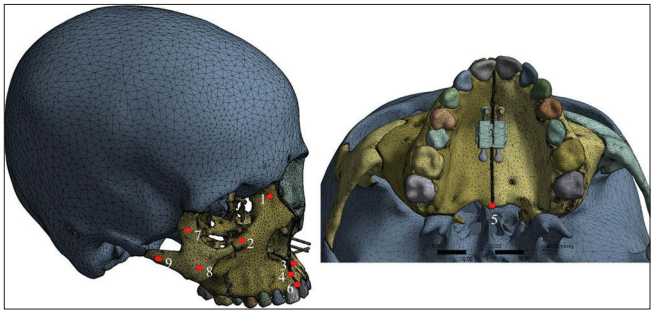

Figure 4: Anatomical landmarks; 1: frontal process of the maxilla, 2: inferior orbital rim, 3: ANS, 4: Point A, 5: PNS, 6: prosthion, 7: frontal process of the zygoma, 8: maxillary process of the zygoma and 9: temporal process of the zygoma

force vector of 500 g per side was directed 30° inferior to the occlusal plane.[9]

The maxillofacial bones displacement at a few anatomical landmarks [Figure 4] i.e. the frontal process of the maxilla, inferior orbital rim, anterior nasal spine (ANS), Point A, prosthion, frontal process of the zygoma, maxillary process of the zygoma, temporal process of the zygoma, and posterior nasal spine (PNS) were used to compare the displacement (mm) at each position in the X, Y, and Z directions. The stress distribution on the circummaxillary sutures [Figure 5], i.e., the frontomaxillary, internshala, pterygomaxillary, nasomaxillary, zygomaticotemporal, zygomaticofrontal, and zygomaticomaxillary sutures, as well as the midpalatal sutures, were evaluated using the Von-Mises stress calculation.

Superimposition was done to study the skeletal displacement as a result of changing the appliance design. According to the 3D coordinates, the unloaded model (without applied force) was at the bottom, and the loaded model (with applied force) was on top of it. As the 3D FEA model was produced using a 3D coordinate system, all anatomical structures were a best-fit superimposition. The same local

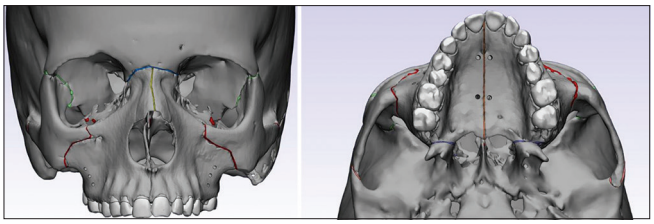

Figure 5: Circummaxillary sutures (colour coded): Frontomaxillary suture- Blue, Internasal suture -Yellow , Zygomaticomaxillary suture -Red, Zygomaticofrontal sutures -Green, Zygomaticotemporal suture – Pink, Pterygomaxillary suture -Purple, Midpalatal sutures - Brown: Midpalatal sutures

3D coordinate system and amplification coefficient were established to make the deformation of the 3D models visible directly.

Results

A comparison of the displacement pattern in X, Y, and Z-axis is shown in Figure 6.

Transverse plane

The displacement along the transverse plane is shown in X axis [Table 2]. All landmarks in the transverse plane, with the exception of the PNS and the temporal process of the zygoma, showed outward movement and also showed a V-shaped expansion pattern in all four-appliance design used in this study. However, Type II appliance design showed an apparently symmetrical displacement of all the landmarks.

The inferior orbital rim experienced the greatest transverse displacement in the Type I and Type III, which used palatal protraction force, whereas the frontal process of the zygoma and prosthion, respectively, experienced the greatest displacement in the Type II and Type IV, which used buccal protraction force.

The landmark prosthion exhibited the least displacement in Type I, whereas Point A exhibited the least displacement in Type II and Type III, despite both points being anatomically close to one another. The frontal process of the zygoma experienced the least displacement in Type IV appliance design, which used two screws and a buccal protraction force.

Sagittal plane

The displacement along the sagittal plane is shown in Y axis [Table 3]. In the sagittal plane, most of the landmarks in Types I, II, III, and IV exhibited a considerable forward movement. All the landmarks in the nasomaxillary complex migrated forward, except for PNS in Type I and III appliance design and the frontal process of maxilla in Type II appliance design. In Type IV appliance design ANS, Point A, PNS, and prosthion were the only landmarks that showed a forward movement, while the frontal process of maxilla, inferior orbital rim, frontal process of zygoma, maxillary process of zygoma, and temporal of zygoma

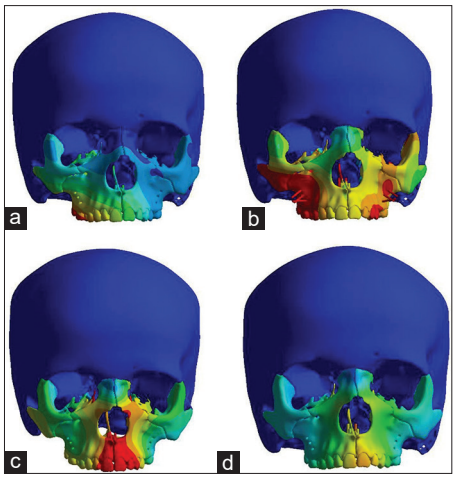

Figure 6: Three-dimensional finite element method of the craniomaxillary complex showing displacement; (a) Type I, (b) Type II, (c) Type III, (d) Type IV

Table 1: Material properties of components used in study

Material	Young's modulus (MPa)	Poisson's ratio
Cortical bone	1.37×10^4	0.30
Cancellous bone	7.9×10^3	0.30
Suture	10	0.49
Periodontal ligament	50.00	0.49
Tooth	2.07×10^4	0.30
Mini plates	1.05×10^5	0.33
Mini screw	1.05×10^5	0.33
Expander	190,000	0.33

showed backward movement. This backward movement may be due to the clockwise rotation of the maxilla.

The frontal process of the maxilla moved the highest in Type III and the least in Type II. The temporal process of the zygoma in Type I and Type III, the maxillary process of the zygoma in Type II, and the prosthion in Type IV showed the greatest amount of forward movement. The least amount of forward movement was seen in PNS in Type I and III, frontal process of maxilla in Type II, and maxillary process of zygoma in Type IV.

Vertical plane

The displacement along the vertical plane is shown in Z axis [Table 4]. All the landmarks in Type I, II, and III appliance design moved downward except ANS, point A, and prosthion, while in Type IV appliance design ANS and point A moved upward whereas PNS moved downwards. This demonstrates there is a clockwise rotation of maxilla in Type I, II, and III and a counterclockwise rotation in Type IV.

In Type I appliance design, the downward displacement was greatest at ANS and least at the frontal process of zygoma. The downward movement at anterior points ANS, Point A, and prosthion was of the same magnitude, while that of posterior point PNS was found to be less when

Table 2: Transverse displacement (mm) of landmarks

Landmarks	Type 1	Type 2	Type 3	Type 4
Frontal process of maxilla	−0.072	−0.018	−0.074	−0.011
Inferior orbital rim	−0.156	−0.019	−0.149	−0.012
ANS	−0.037	−0.017	−0.042	−0.031
Point A	−0.014	−0.009	−0.018	−0.026
PNS	0.080	0.073	0.105	0.027
Prosthion	−0.011	−0.015	−0.019	−0.040
Frontal process of zygoma	−0.113	−0.038	−0.096	−0.026
Maxillary process of zygoma	−0.076	0.002	−0.061	−0.007
Temporal process of zygoma	0.030	0.025	0.052	0.011

ANS: Anterior nasal spine; PNS: Posterior nasal spine

Table 3: Sagittal displacement (mm) of landmarks

Landmarks	Type 1	Type 2	Type 3	Type 4
Frontal process of maxilla	−0.008	0.001	−0.013	0.004
Inferior orbital rim	−0.042	−0.013	−0.048	0.007
ANS	−0.045	−0.024	−0.065	−0.029
Point A	−0.034	−0.022	−0.052	−0.033
PNS	0.016	−0.003	0.015	−0.017
Prosthion	−0.012	−0.017	−0.024	−0.033
Frontal process of zygoma	−0.076	−0.011	−0.074	0.007
Maxillary process of zygoma	−0.061	−0.028	−0.061	0.002
Temporal process of zygoma	−0.087	−0.013	−0.087	0.009

ANS: Anterior nasal spine; PNS: Posterior nasal spine

compared to the anterior points depicting a clockwise rotation of the maxilla.

In Type II, the downward displacement was greatest at the temporal process of zygoma and least at the frontal process of zygoma. The downward movement of anterior points ANS, Point A, and prosthion was of the same magnitude, while that of posterior point PNS was found to be less. The downward movement of anterior and posterior points was less than that of Type I, which suggests that there was lesser rotation of maxilla when compared to Type I.

In Type III appliance, the downward displacement was greatest at ANS and least at frontal process of zygoma, which is similar to Type I appliance. The downward movement of anterior points ANS, Point A, and prosthion were of same magnitude and similar to that of Type I, whereas the downward movement of posterior point PNS is less than that of the anterior point and lesser than that of Type I. The above result showed that the rotation of maxilla in clockwise direction is greater in Type III when compared to Types I and II.

In Type IV, the anterior points Point A, prosthion, and ANS had moved upward and the posterior point PNS had moved downward. Therefore, in Type IV, the maxilla had a counterclockwise rotation, which was opposite to the movement noted in Types I, II, and III.

The stress distribution in sutures is shown in Figure 7 and Table 5. The distribution of stress is depicted in the figure's color scale, which ranges from lowest (blue) to greatest (red).

Table 4: Vertical displacement (mm) of landmarks

Landmarks	Type 1	Type 2	Type 3	Type 4
Frontal process of maxilla	−0.055	−0.013	−0.045	−0.001
Inferior orbital rim	−0.109	−0.034	−0.101	−0.011
ANS	−0.257	−0.050	−0.259	0.003
Point A	−0.252	−0.049	−0.247	0.003
PNS	−0.244	−0.038	−0.158	−0.082
Prosthion	−0.255	−0.051	−0.249	0.004
Frontal process of zygoma	−0.014	−0.002	0.004	−0.004
Maxillary process of zygoma	−0.031	−0.028	−0.010	−0.020
Temporal process of zygoma	−0.052	−0.066	−0.063	−0.059

ANS: Anterior nasal spine; PNS: Posterior nasal spine

Table 5: Stress distribution (MPa) in sutures

Landmarks	Type 1	Type 2	Type 3	Type 4
Frontomaxillary suture	16.23	4.81	14.1	0.98
Internasal suture	3.69	1.39	3.26	0.36
Pterygomaxillary suture	2.62	2.17	2.78	2.90
Zygomaticofrontal suture	3.48	2.27	2.32	0.66
Zygomaticomaxillary suture	2.0	3.14	2.91	0.51
Zygomaticotemporal suture	2.48	1.52	3.01	1.25
Midpalatal suture	3.48	1.78	3.77	1.59

In Type I, the highest stress is around the frontomaxillary suture, which is greater than in Types II, III, and IV. A steep reduction in stress were observed in other sutures namely, internasal suture, midpalatal suture, zygomaticofrontal suture, pterygomaxillary suture, zygomaticotemporal suture, and zygomaticomaxillary suture in descending order.

In Type II, the greatest stress is around the frontomaxillary suture but is less than that in Types I and III. A gradual reduction in stress was observed in other sutures namely, zygomaticomaxillary suture, zygomaticofrontal suture, pterygomaxillary suture, midpalatal suture, zygomaticotemporal suture, and internasal suture in descending order. The least stress is around the internasal suture, and the stress around all the sutures except zygomaticomaxillary suture is less than that of in Types I and III.

The greatest stress in Type III appliance design was around the frontomaxillary suture, which was less than that of Type I appliance design but greater than in Types II and IV appliance design. A steep reduction in stress was observed in other sutures such as midpalatal suture, internasal suture, zygomaticotemporal suture, zygomaticomaxillary suture, pterygomaxillary suture, and zygomaticofrontal suture in descending order.

Type IV appliance design exhibited the greatest stress around the pterygomaxillary suture than all other appliance designs. A gradual reduction in stress was observed in other sutures such as internasal suture, zygomaticomaxillary

suture, zygomaticofrontal suture, frontomaxillary suture, zygomaticotemporal suture, and midpalatal suture in descending order. The stress around all the sutures except in pterygomaxillary suture is the least in Type IV appliance design.

Therefore, Types I, II, and III appliance design resulted in a higher stress distribution towards the superior structures of the maxilla whereas the Type IV appliance design resulted in higher stress distribution toward the inferior structures of the maxilla.

Superimposition

Each simulation's superimpositions were generated. The "after" image is shown in a variety of colors that precisely match the amount of y-displacement (Protraction) and Z displacement (rotation) after force application, while the "before" image is exhibited in opaque shadow for the superimpositions [Figure 8].

Discussion

Maxillary protraction with a facemask has proven to be a successful treatment option for correction of Class III malocclusion with maxillary deficiency. In addition to the anteroposterior divergence, a transverse variance also contributes to a reduction in maxillary growth, which frequently results in posterior crossbites. According to Haas, the orthopedic effect of RME resulted in a forward and downward shifting of the maxilla and a concurrent clockwise rotation of the mandible. In addition, he had also reported on the remodeling effect of circummaxillary suture with the RME-FM combination.[10] According to Turley, expansion of the palate disarticulates the maxilla and causes cellular responses in these circummaxillary suture, which enables a more favorable response to protraction forces.[11]

The protraction of the maxilla with a miniplate in the infra-zygomatic crest area requires an invasive flap surgery for placement and removal of the miniplate. On the contrary, the palatal plate can be attached to the MARPE, and placement is done as a flapless procedure with no risk to the vital structures.[12-14]

In the previous studies, when only skeletal protraction was done without RME, it resulted in a counterclockwise rotation of the maxilla.[15-18] In our study, when protraction was combined with skeletal expansion, it resulted in a forward and downward displacement of the maxilla in Type I, II, and III appliance design, which is indicated by the downward displacement of anterior point (ANS, point A, and prosthion) and upward displacement of posterior point (PNS) and is in consistent with the previous studies when protraction was combined with expansion.[12,15,19-21]

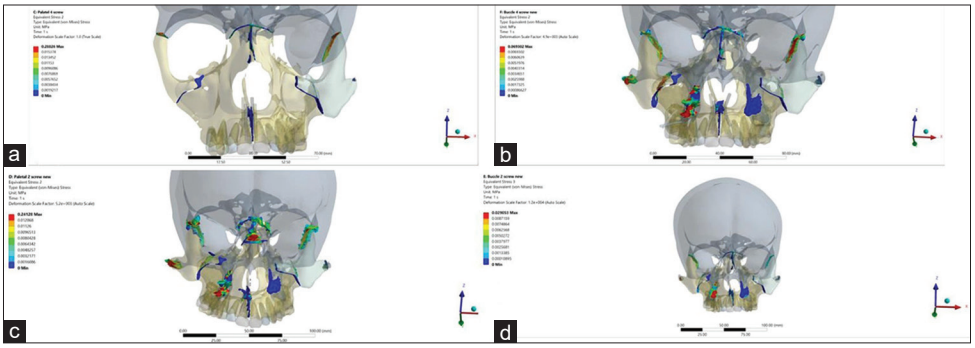

Figure 7: Three-dimensional finite element method of the craniofacial sutures showing stress distribution. (a) Type I, (b) Type II, (c) Type III and (d) Type IV

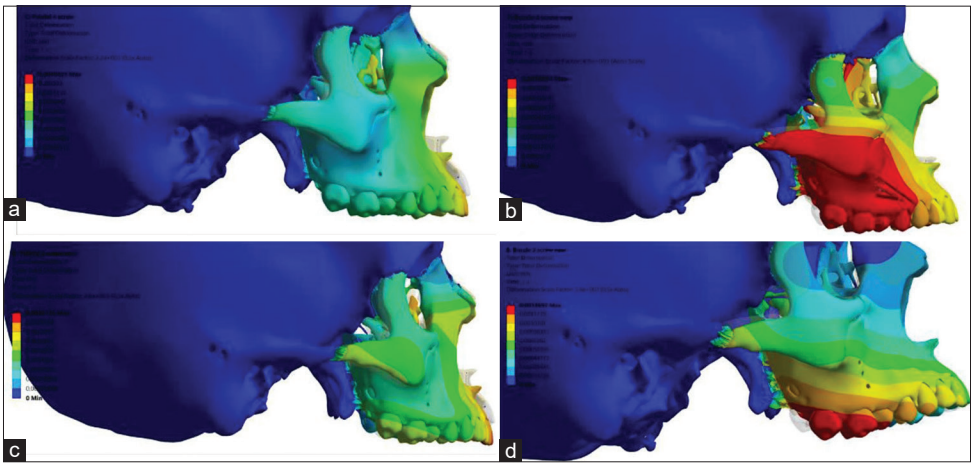

Figure 8: Superimposition. Before: Opaque, After: Variety of colors. (a) Type I, (b) Type II, (c) Type III and (d) Type IV

Even with expansion, the maxilla in Type IV appliance design rotated anticlockwise and moved forward, indicated by the upward displacement of anterior point (ANS, point A, and prosthion) and downward displacement of posterior point PNS, which was consistent with the previous studies.[19,22-25] Yan *et al*.[26] studied the effects of maxillary protraction on the craniomaxillary complex with bone anchorage in the infrazygomatic buttresses and dental anchorage in the maxillary first molars. They observed that when the force direction was around 30° in the bone anchoring model and dental anchorage model, the craniomaxillary complex could move in a nearly translatory fashion in dental anchorage and with very mild clockwise rotation in bone anchorage.

In our study, Type II with buccal protraction and RME experienced the least clockwise rotation, which was consistent with the previous studies reported by Suresh *et al*.[12] and Garg *et al*.[27] In Type I and Type III appliance design, the displacement trends were apparently symmetrical to each other in a clockwise direction. This may be due to the fact that Type I and III appliance design used the same point of force application (palatal hooks positioned between the canine and first premolar), which is anterior and inferior to the center of resistance of the maxilla. In type IV appliance design, the force application is between canine and premolar on the buccal side, which is also anterior and inferior to center of resistance but superior to that of Types I and III appliance design this might be the reason for the counterclockwise rotation seen in type IV appliance design. Hence, further studies with increase in the degree of force vector need to be conducted to check its influence on the rotation of maxilla. The amount of forward displacement was also higher as in previous studies when the palatal plates were employed for protraction.[15,17,28,29]

Previous investigations have noted anterior maxillary constriction following maxillary protraction with face mask, which supports a necessity for maxillary expansion with protraction.[10,24] The activation of MARPE produced an anteroposterior expansion pattern in triangular shape, with the triangle's apex pointing posteriorly in all the appliance design (Type I, Type II, Type III, and Type IV). The highest resistance to expansion was in the pterygomaxillary process, and this was consistent with the previous studies by Suresh *et al*.[12] and Lee *et al*.[8] The nasomaxillary complex was modeled as isotropic, homogeneous and continuous without suture grids in many earlier research. This would lead to an error when assessing the distribution of stress in sutures. Nonetheless, distinct sutural grids were made as in previous study by Suresh *et al*.,[12] and as a result, the stress distribution in sutures may be more exact, allowing for the implementation of these findings as guidelines in therapeutic settings. The sutures play a significant role in the development of craniofacial region. The sutures carry mechanical stress from the external forces acting on the maxilla that reach distant structures in the craniofacial regions, which is quantified as sutural strain.[30] Previous researchers found that maxillary protraction caused considerable alterations in the circummaxillary sutures.[2,31] In our study, the palatal protraction type demonstrated the greatest stress in circummaxillary sutures, which explains the increased forward movement in these two Type I and Type II appliance design, and this was consistent with the previous study by Kim *et al*.[17] The suture with the highest von Mises stress was the frontomaxillary suture in Types I, II, and III appliance design and pterygomaxillary suture in Type IV appliance design.

The findings of our finite element study on the right and left sides are slightly asymmetric as a result of the asymmetry in the arch form. Since such movements will be constrained by the surrounding anatomical structures, this has little impact on the clinical situation. Due to the maxilla's tendency to rotate anticlockwise direction as well, maxillary protraction is typically not recommended in patients with Class III and open bite.[12] The therapeutic significance of this research is that it shows that in patients with skeletal Class III malocclusion and open bite predisposition or hyperdivergent development pattern, maxillary protraction produces good results with Types I, II, and III appliance design and maxillary protraction with Type IV appliance design in Class III with hypodivergent pattern. However, clinical application of these appliance designs may be necessary to verify the results of this FEA since it is a brief evaluation of the force application.

Conclusion

Our finite element study on the application of MARPE-assisted maxillary protraction recommends:

- Maxillary expansion with protraction from a palatal plate (Type I and III) produced more effective results than buccal plate designs (Type II and III)
- In skeletal Class III with open bite, the recommended design is MARPE design Type I, II, and III
- In skeletal Class III with deep bite, the recommended design is MARPE design type IV
- FEM studies provide a guideline on designing force application and appliance design. The recommended designs are expected to improve the clinical management of skeletal Class III.

Financial support and sponsorship

Nil.

Conflicts of interest

There are no conflicts of interest.

References

1. Papadopoulou AK, Koletsi D, Masucci C, Giuntini V, Franchi L, Darendeliler MA. A retrospective long-term comparison of

early RME-facemask versus late hybrid-hyrax, alt-RAMEC and miniscrew-supported intraoral elastics in growing class III patients. Int Orthod 2022;20:100603.
2. Gautam P, Valiathan A, Adhikari R. Maxillary protraction with and without maxillary expansion: A finite element analysis of sutural stresses. Am J Orthod Dentofacial Orthop 2009;136:361-6.
3. Nartallo-Turley PE, Turley PK. Cephalometric effects of combined palatal expansion and facemask therapy on class III malocclusion. Angle Orthod 1998;68:217-24.
4. Liou EJ. Effective maxillary orthopedic protraction for growing class III patients: A clinical application simulates distraction osteogenesis. Prog Orthod 2005;6:154-71.
5. Wilmes B, Nienkemper M, Drescher D. Application and effectiveness of a mini-implant- and tooth-borne rapid palatal expansion device: The hybrid hyrax. World J Orthod 2010;11:323-30.
6. Fricke-Zech S, Gruber RM, Dullin C, Zapf A, Kramer FJ, Kubein-Meesenburg D, *et al.* Measurement of the midpalatal suture width. Angle Orthod 2012;82:145-50.
7. Meng WY, Ma YQ, Shi B, Liu RK, Wang XM. The comparison of biomechanical effects of the conventional and bone-borne palatal expanders on late adolescence with unilateral cleft palate: A 3-dimensional finite element analysis. BMC Oral Health 2022;22:600.
8. Lee HK, Bayome M, Ahn CS, Kim SH, Kim KB, Mo SS, *et al.* Stress distribution and displacement by different bone-borne palatal expanders with micro-implants: A three-dimensional finite-element analysis. Eur J Orthod 2014;36:531-40.
9. Ngan PW, Hagg U, Yiu C, Wei SH. Treatment response and long-term dentofacial adaptations to maxillary expansion and protraction. Semin Orthod 1997;3:255-64.
10. Haas AJ. The treatment of maxillary deficiency by opening the midpalatal suture. Angle Orthod 1965;35:200-17.
11. Turley PK. Orthopedic correction of class III malocclusion with palatal expansion and custom protraction headgear. J Clin Orthod 1988;22:314-25.
12. Suresh S, Sundareswaran S, Sathyanadhan S. Effect of microimplant assisted rapid palatal expansion on bone-anchored maxillary protraction: A finite element analysis. Am J Orthod Dentofacial Orthop 2021;160:523-32.
13. Nienkemper M, Wilmes B, Pauls A, Drescher D. Maxillary protraction using a hybrid hyrax-facemask combination. Prog Orthod 2013;14:5.
14. Kook YA, Bayome M, Park JH, Kim KB, Kim SH, Chung KR. New approach of maxillary protraction using modified C-palatal plates in class III patients. Korean J Orthod 2015;45:209-14.
15. Gautam P, Valiathan A, Adhikari R. Skeletal response to maxillary protraction with and without maxillary expansion: A finite element study. Am J Orthod Dentofacial Orthop 2004;135:723-8.
16. Lee NK, Baek SH. Stress and displacement between maxillary protraction with miniplates placed at the infrazygomatic crest and the lateral nasal wall: A 3-dimensional finite element analysis. Am J Orthod Dentofacial Orthop 2012;141:345-51.
17. Kim KY, Bayome M, Park JH, Kim KB, Mo SS, Kook YA. Displacement and stress distribution of the maxillofacial complex during maxillary protraction with buccal versus palatal plates: Finite element analysis. Eur J Orthod 2015;37:275-83.
18. Keles A, Tokmak EC, Erverdi N, Nanda R. Effect of varying the force direction on maxillary orthopedic protraction. Angle Orthod 2002;72:387-96.
19. Moon W, Wu KW, MacGinnis M, Sung J, Chu H, Youssef G, *et al.* The efficacy of maxillary protraction protocols with the micro-implant-assisted rapid palatal expander (MARPE) and the novel N2 mini-implant-a finite element study. Prog Orthod 2015;16:16.
20. Park JH, Bayome M, Zahrowski JJ, Kook YA. Displacement and stress distribution by different bone-borne palatal expanders with facemask: A 3-dimensional finite element analysis. Am J Orthod Dentofacial Orthop 2017;151:105-17.
21. Rai P, Garg D, Tripathi T, Kanase A, Ganesh G. Biomechanical effects of skeletally anchored class III elastics on the maxillofacial complex: A 3D finite element analysis. Prog Orthod 2021;22:36.
22. Borzabadi-Farahani A, Lane CJ, Yen SL. Late maxillary protraction in patients with unilateral cleft lip and palate: A retrospective study. Cleft Palate Craniofac J 2014;51:e1-10.
23. Liu C, Zhu X, Zhang X. Three-dimensional finite element analysis of maxillary protraction with labiolingual arches and implants. Am J Orthod Dentofacial Orthop 2015;148:466-78.
24. Vaughn GA, Mason B, Moon HB, Turley PK. The effects of maxillary protraction therapy with or without rapid palatal expansion: A prospective, randomized clinical trial. Am J Orthod Dentofacial Orthop 2005;128:299-309.
25. Ngan P, Yiu C, Hu A, Hägg U, Wei SH, Gunel E. Cephalometric and occlusal changes following maxillary expansion and protraction. Eur J Orthod 1998;20:237-54.
26. Yan X, He W, Lin T, Liu J, Bai X, Yan G, *et al.* Three-dimensional finite element analysis of the craniomaxillary complex during maxillary protraction with bone anchorage versus conventional dental anchorage. Am J Orthod Dentofacial Orthop 2013;143:197-205.
27. Garg D, Rai P, Tripathi T, Kanase A. Effects of different force directions of intra-oral skeletally anchored maxillary protraction on craniomaxillofacial complex, in class III malocclusion: A 3D finite element analysis. Dental Press J Orthod 2023;27:e2220377.
28. Yu HS, Baik HS, Sung SJ, Kim KD, Cho YS. Three-dimensional finite-element analysis of maxillary protraction with and without rapid palatal expansion. Eur J Orthod 2007;29:118-25.
29. Baik HS. Clinical results of the maxillary protraction in Korean children. Am J Orthod Dentofacial Orthop 1995;108:583-92.
30. Mao JJ. Mechanobiology of craniofacial sutures. J Dent Res 2002;81:810-6.
31. Tanaka OM, Saga AY, Pithon MM, Argenta MA. Stresses in the midpalatal suture in the maxillary protraction therapy: A 3D finite element analysis. Prog Orthod 2016;17:8.